Proceedings World Geothermal Congress 2020+1
Reykjavik, Iceland, April - October 2021

Investigation on heat transfer characteristics in super-long gravity-assisted heat pipe for the purpose of deep geothermal energy exploitation

Juanwen Chen, Jiwen Cen, Wenbo Huang, Fangming Jiang

Laboratory of Advanced Energy Systems, Guangdong Key Laboratory of New and Renewable Energy Research and Development, CAS Key Laboratory of Renewable Energy, Guangzhou Institute of Energy Conversion, Chinese Academy of Sciences (CAS), Guangzhou 510640, China

E-mail: fm_jiang2000@yahoo.com

Keywords: Deep geothermal energy; Geothermal energy exploitation; Hot dry rock; Super- or extra- long heat pipe; Multiphase flow

ABSTRACT

The exploitation of deep geothermal energy has created a great demand for super-long distance heat transportation technology. Heat pipe is capable of transferring heat very effectively from its high to the low temperature end relying on the working fluid phase transitions. We proposed using super-long gravity-assisted heat pipe to exploit earth-deep geothermal energy. The heat pipe that can be used for earth-deep geothermal energy exploitation differs from its normal size (less than 10 m long) counterparts that have been widely used in various industries due mainly to the extremely large length-to-diameter ratio. This geometric characteristic may significantly affect the multiphase flow and heat transfer inside the heat pipe. In this work, a systematic experimental study on the multiphase flow regimes and the performance of an extra-long heat pipe was conducted. The experimental heat pipe has a length-to-inner diameter ratio (L/D=40 m/7 mm =5714), which mimics the major geometric characteristic of real super-long geothermal heat pipes. Particular focus of the present work was placed on correlating the heat transfer performance of the heat pipe with the multiphase flow regimes inside. The thermal performance of the experimental heat pipe was found to be significantly affected by the depth of liquid pool accumulated at the bottom and can be correlated with four different multiphase flow regimes inside. The transition between these flow regimes is closely related to the properties of working fluid and the fluid fill height. It is noteworthy that the correlation of heat pipe thermal performance and the multiphase flow inside is quite different from that for normal size heat pipes. Besides too deep liquid pool, the experimental results suggest as well the liquid dry-out operation must be avoided for real geothermal heat pipes.

1. INTRODUCTION

In recent years, with the development of geothermal energy utilization, it is essential to expand the utilization of geothermal energy into the middle and deep layers underground.

Hot dry rock (HDR), a vast store of thermal energy that is contained in the hot impervious crystalline basement rocks, was found to occupy more than 90% of the total US geothermal resource. Aiming to extract the energy stored in HDR, the prototype of an Enhanced Geothermal System (EGSs) was designed and implemented by the Los Alamos National Laboratory in the 1970s. However, in spite of the huge invest and research on EGSs, so far significant financial risks still exist for EGS projects since it remain as a major challenge to effectively control the quality of the fractures' network in EGS reservoir, which to a great extent determines the production potential of the EGS[1]. Some practical issues also lead to operation and maintenance costs, such as corrosion and scaling in wellbores and power plant components, and the loss of working fluid while circulating[2].

This has inspired an active demand for other super-long-distance heat transportation technology. In 2017, the technology using a super-long gravity-assisted heat pipe to acquire the deep geothermal energy from the deep underground to above ground has been proposed and preliminarily evaluated by Jiang et al.[3, 4]. This technology is soon considered as a promising technology, because it can avoid the problems existing in the EGSs, including the loss of working fluid, the corrosion of equipment, and the huge cost in building the artificial reservoir.

Heat pipe is capable of transferring heat very effectively from its high to the low temperature end relying on the working fluid phase transitions[5, 6]. It consists of an evaporator absorbing heat, an adiabatic section transporting heat, and a condenser releasing heat. Once the liquid reaches its saturation temperature at the evaporator, it evaporates into vapor which flows to the condenser and delivers its latent heat to the coolant at the condenser. After the vapor condenses, the condensate working fluid returns to the evaporator by gravity (wickless heat pipes) or by capillary force (wicked heat pipe). When the evaporator is positioned at the lower part of the gravitation field, the heat pipes do not need wicking to return the condensate working fluid from the condenser to the evaporator due to gravity. Based on the cyclic evaporation and condensation of working fluid, the heat pipes utilize the latent heat of the phase change instead of conduction or convection. A large quantity of heat can be transferred from the evaporator end to the condenser end with a relatively small temperature difference between them. Thus, the heat pipes have high thermal conductance.

Despite the relatively simple design and geometry, the thermodynamics of gravity-assisted heat pipe is quite complex. The normal lengths of heat pipe are usually less than 10 m, while the heat pipe used to obtain the deep geothermal energy has to be a few kilometers long. Due to the large length-to-diameter ratio (>104), the multiphase flow coupled with the phase change inside the super-long heat pipe is even more complicated. It exhibits fickle flow regimes rather than the stable high-efficiency nucleating boiling as the normal heat pipe[7].

For normal size heat pipes, a number of experimental studies have already been carried out to provide data on heat pipe operation, validation of theoretical models, and databases for design[8]. In addition, many theoretical analyses have incorporated empirical or semi-empirical correlations to simplify the models and the solution process. For a heat pipe working in the designed operation, the heat transfer coefficient of the condenser is normally derived from the Nusselt solution for film-wise condensation, while that of the evaporator is derived from the solution for nucleating boiling[9]. Different from the general operation design situation, the multiphase flow inside a heat pipe is not always in the stable phase-changing state [10]. The application of heat pipe is hindered in some cases by the geyser boiling [11-14] or by various other factors such as dry-out of liquid film and flooding of counter-current liquid-vapor flow [15, 16].

While the effects of such unsteady flow characteristics can most likely be neglected or easily avoided for normal pipes, they must be considered in the design of super-long heat pipe. This is particularly true regarding the operating limitations, because such a large aspect ratio may have a significant effect on the heat transfer limit when the hydraulic characteristics are considered. It is significant to keep the super-long heat pipe working in a suitable multiphase flow status for the high-efficiency of phase change. At present, the intrinsic connection of the multiphase flow status and thermal performance of super-long heat pipe is still not well understood. It is necessary to recognize the transition of flow status inside the super-long heat pipe.

The aim of this work is to experimentally study the relationship between multiphase flow regime and the performance of super-long heat pipe. A large length-to-inner-diameter ratio heat pipe (>5000) was built for the experimental tests. By the measurement and analysis of performance and the evolution and distribution of surface temperature along the heat pipe, the transition of multiphase flow regimes is identified. Moreover, the relationship between the flow regimes and the performance of super-long heat pipe is carefully investigated. The flow regimes and thermal performance of the super-long heat pipe using water, ethanol and R134a as working fluid were compared to explore the reason of the influence of working fluid on the thermal performance. Please be very careful to use styles throughout the document, so that all the papers will have a similar appearance. Normal text is in <Normal Style>

2. EXPERIMENT SYSTEM

In order to study the correlation between the multiphase flow regime and the performance of super-long heat pipe, an experimental apparatus consisting of a heat pipe with length-to-inner-diameter ratio of more than 5000 was designed and constructed, as illustrated in Figure 1. A closed copper tube with dimensions of 40 m length, 7 mm inner diameter and 1.5 mm thickness, was used as the wickless gravity-assisted heat pipe. The heat pipe was designed to be divided into three sections: the lower 20 m part is the evaporator section, the middle 15 m part is the adiabatic section and the upper 5 m is the condenser section. In the evaporator, heat was supplied by five groups of electrical heating wrapped around the evaporator. The heat flux was controlled by adjusting the output voltage of the transformers and was measured using multimeters and wattmeters. In the condenser, a polycarbonate tube with 20 mm diameter and 5 m length was employed as a water jacket. The coolant water flowed into the bottom of the water jacket and outflowed from the top, carrying off the heat from the condenser. The flow rate was controlled by adjusting the liquid level of a tank. In order to approach to the possible thermal insulation conditions in the actual geothermal well, the entire pipe was wrapped with thermal insulation material (heat conductivity coefficient is 0.04 $W \cdot m^{-1} \cdot K^{-1}$) which was 15 mm in thickness.

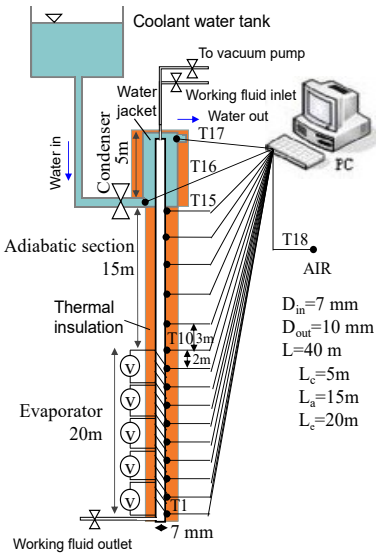

Figure 1: Experimental system

To facilitate adding and replacing the working fluid, the top and bottom of the heat pipe were designed to be operable vents. The bottom of the heat pipe was connected with a valve through a stainless-steel tube with 2 mm diameter and thickness of 1.5 mm, so that the working fluid can flow out controllably. The top was connected with a stainless-steel tube. For the requirement of operation, two vacuum valve were used to connect the tube with a vacuum pump and a working fluid tank respectively. The vacuum pump was employed to produce vacuum condition inside the heat pipe, while the working fluid tank was used to supply working fluid.

Eighteen T-type thermocouples were used to monitor the temperature at different positions. Fifteen of them ($T_1 \sim T_{15}$) were fixed on the outer surface of the heat pipe: 11 on the evaporator section ($T_1 \sim T_{11}$) with 2 m equal spacing and 4 on the adiabatic section ($T_{12} \sim T_{15}$) with 3.75 m equal spacing. Two thermocouples (T_{16}, T_{17}) were placed at the inlet and outlet of the water coolant flow at the condenser section, and the last one (T_{18}) was used to measure the ambient temperature.

The uncertainty in the measurement of the temperature readings ($T_1 \sim T_{18}$) is about ± 0.3 K. As most of the temperatures in this experiment are in the range of 30~100 ℃, the relative error is about 0.46% (= 0.3/[(30+100)/2]). The uncertainty in the measured value of the input heat of the evaporator section Q_{in} is about 0.4%. The heat transmitted from the condenser section Q_{out} is equal to the heat absorbed by the coolant water in the jacket, and was calculated by:

$$Q_{out} = \mathrm{C_p} v_c \left(T_{16} - T_{17}\right) \qquad (1)$$

where C_p is the isobaric heat capacity. The uncertainty in measuring the flow rate value v_c is around 0.4%. Therefore, the uncertainty in Q_{out} is:

$$\partial Q_{out} / Q_{out} = \sqrt{\left(\partial T_{16} / T_{16}\right)^2 + \left(\partial T_{17} / T_{17}\right)^2 + \left(\partial v_c / v_c\right)^2} = \sqrt{2 \times 0.46\ \%^2 + 0.4\ \%} = 0.9\ \% \qquad (2)$$

The experiments were performed with ethanol or deionized water or R134a as the heap pipe working fluid as these three fluids are widely used in heat pipes. In each case, all the temperatures were measured every two seconds. Other details of parameters investigated in this experimental study, such as heat input (Q_{in}), fill height (FH) and fill ratio (FR, which is the fill height divided by the evaporator length) are shown in Table 1.

Table 1. The parameters considered in this experimental work

Working fluid	Heat Input Q_{in} (W)	Fill height FH (m)	Fill ratio FR
Deionized water	200~900	2~10	10% ~ 50%
Ethanol	100~500	2~8	10% ~ 40%
Acetone	100~400	6~8	30% ~ 40%

3.RESULTS AND DISCUSSION

3.1 Flow regimes

Figure 2 shows the outflow heat Q_{out} and the transient temperature response of the heat pipe using water as working fluid. As can be seen, the outflow heat increases with the inflow heat. The efficiency (i.e., Q_{out} divided by Q_{in}) of heat transmission is in the range of 30% ~ 40% when the Q_{in} is in the range of 100 W~ 350 W, but lower than 30% when the Q_{in} is higher than 350 W. The heat loss due to the thermal insulation is generally negligible for normal size heat pipe but significant for super-long heat pipe. As shown in the analysis of heat dissipation in our previous research, the heat loss (more than 50%) is attributed to the unavoidable heat release (to the ambient) through the thermal insulation covering the heat pipe. When Q_{in} is less than 100 W, the Q_{out} is almost zero, which means the heat pipe is not started up. Considering the case of FH = 6 m for instance, the surface temperature response shows four different stages with the increase in Q_{in}, as shown in Figure 3a-d.

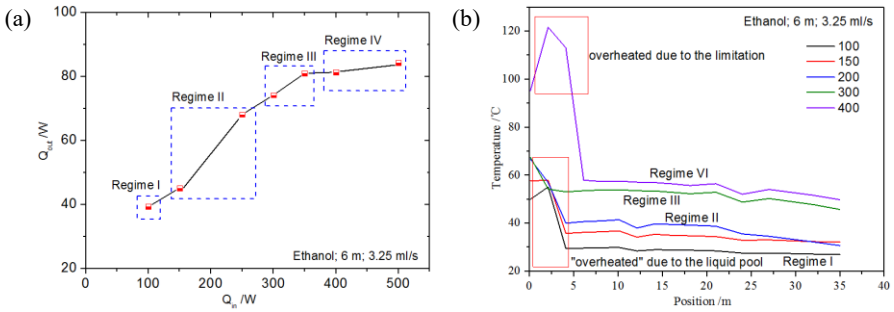

Figure 2: The performance (a) and the stable surface temperature (b) of the heat pipe

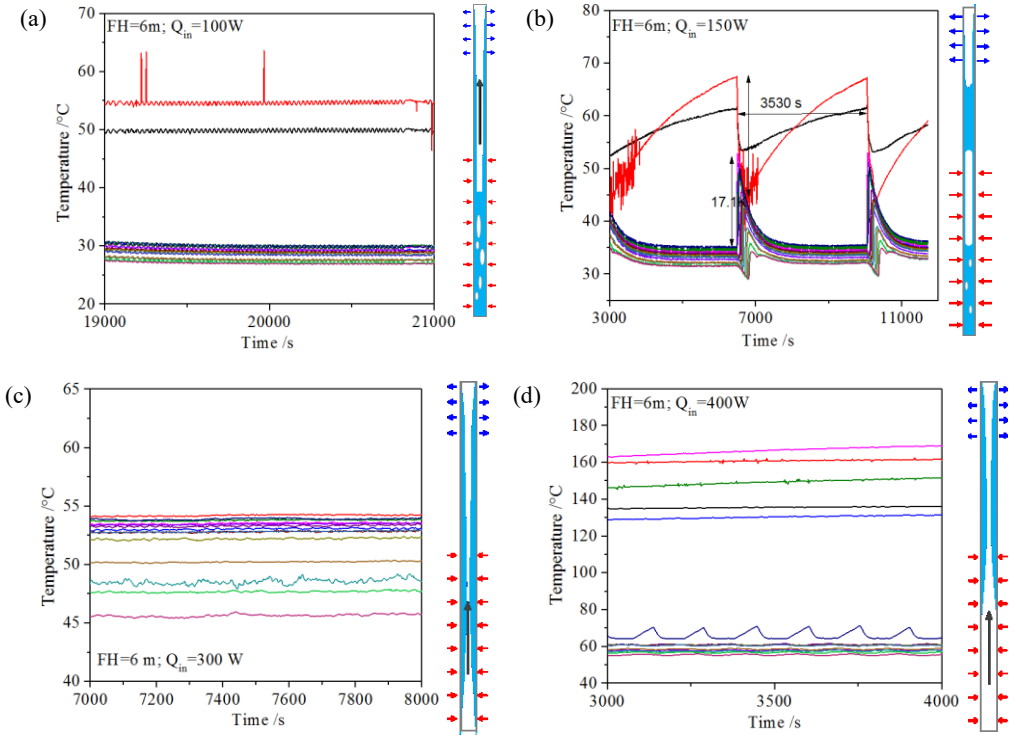

Figure 3: Four regime along with the heat load increase. Temperature evolution on the outer wall of heat pipe during typical (a) Regime I-Nucleating pool boiling regime; (b) Regime II-Geyser boiling regime; (c) Regime III-Evaporating film boiling regime; (d) Regime IV-Overheated boiling regime. FH = 6 m. The inside sketches illustrate the liquid-vapor distribution in each flow regime.

Four different flow regimes of phase change are indicated by these characteristics:

(1) Regime I: Nucleating pool boiling regime

At low Q_{in}, less liquid is evaporated into vapor or flowing on the inner wall of pipe, while most of the liquid is still reserved at the bottom of evaporator as a liquid pool. The liquid pool is in the state of nucleating pool boiling, while the two-phase flow in the evaporator is similar to the quasi-bubbly-flow.

In this regime, the hydrostatic head of the liquid pool is essential for the saturation temperature in the evaporator. The change in liquid level in the pool due to boiling is negligible. Thus, the pressure at the bottom of the pool is:

$$P_{eva}' = P_{sat} + \rho_l g h \qquad (3)$$

where P_{eva}' is the theoretical local evaporation pressure, P_{sat} is the saturation pressure at the top of the evaporation section, ρ_l is the density of working fluid, g is the gravitational acceleration and h is the height of the liquid pool, which is roughly equivalent to the fill height. The theoretical saturation temperature at the bottom of the pool, T_{eva}', is depended on the pressure of the working fluid, P_{sat}. Obviously, the liquid pool is significant for the temperature distribution in this regime. Due to the effect of the hydrostatic head, the saturation temperature of evaporation is high, which limits the rate of evaporation. Figure 2b shows the temperature distribution on the surface of super-long heat pipe and the efficiency of heat transfer. The efficiency of heat transfer in the nucleating pool boiling regime is low, as can be seen. The effect of the hydrostatic head of the liquid pool is dependent on the liquid height. Thus, the liquid pool usually leads to negligible or slight difference in normal heat pipe. However, in the super-long heat pipe, it has a great effect due to the relatively large liquid height. Notably, liquid height of several meters can enlarge the saturated temperature by dozens of degrees. It would be even more significant for the working fluid whose saturated temperature is sensitive to the pressure.

(2) Regime II: Geyser boiling regime

With the increase in Q_{in}, the surface temperature of the heat pipe begins to fluctuate. As shown in Figure 3b, this periodic fluctuation occurs from T_2 first, followed by T_3 to T_{15} successively. However, T_2 and T_1 show reverse fluctuation direction compared with others. It is because that the liquid level is below the T_3 position. These kinds of fluctuations indicate the typical geyser boiling phenomenon (GBP), which is illustrated in Figure 4.

As Q_{in} increases, the evaporation of the liquid pool in the evaporator is enhanced. The formed bubbles in the liquid pool increase. This increases the possibility of coalescence and the sudden explosive growth of bubble, which leads to the formation of a long large bubble due to the limited space. The long bubble floats and keeps growing due to the evaporation and coalescence, leading to a quasi-

slug-flow. The liquid on top of the bubble is lifted towards the condenser by the pressure of bubble. Subsequently, the growing bubble reaches the liquid level and breaks up, and the relatively cool liquid returns back to the evaporator by gravitational force. After the returned liquid takes some time to be heated to be hot enough, another long bubble forms again, perpetuating the cycle. As a result of this liquid-gas periodic flow, the temperature on the surface of the heat pipe also fluctuates accordingly, which is shown in Figure 3c. The geyser boiling phenomenon relieves the temperature difference caused by the liquid pool, as shown in Figure 4. On average, the temperature along the heat pipe becomes more uniform compared to the nucleating pool boiling regime. In addition to the effect on the heat transmission, it is worth noting that this fast-moving liquid may produce a considerable mechanical vibration accompanied by a loud sound. This may be due to the large fluctuation amplitude of the pressure rise in the channel along with the GBP.

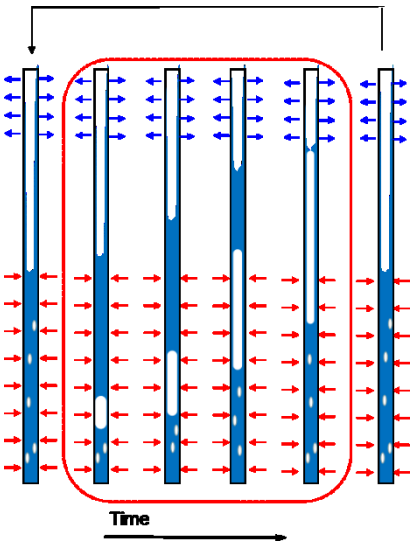

Figure 4: Evolution of a geyser boiling bubble.

(3) Regime III: Evaporation film boiling regime

When the Q_{in} continues to increase, the liquid pool is finally depleted due to the increasingly fast evaporation. Most of the liquid flows on the inner wall of the heat pipe after being condensed. The condensate liquid is completely evaporated just before or after it reaches the bottom of the heat pipe. The two-phase flow in the interior heat pipe is similar to annular gas-liquid countercurrent flow (Figure 3c). There is neither obvious temperature variation due to the liquid pool, nor dry-out section. The whole evaporation section works in evaporation film boiling regime with a high heat transfer coefficient. The temperature difference along the heat pipe is mostly due to the decrease in saturation vapor pressure caused by energy consumption of the vapor after the long-distance gas-liquid counter flow. Therefore, the temperature along the heat pipe is relatively small and the performance of heat transmission is generally higher than that of other regimes, as shown in Figure 4.

Considering the case of FH = 6 m, the film of working fluid should be less than 300 um on average assuming that the liquid covers the inner wall uniformly. Obviously, it is difficult to establish such a smooth film of liquid on the whole inner surface of the pipe because of the surface tension and the vapor-liquid countercurrent flow. It is likely that the liquid film breaks up into a series of rivulets with some dry patches in between, as indicated by previous research [17]. This decreases the heat transfer coefficient of the evaporation to some extent. This regime is maintained only in a narrow operating condition and can easily shift into the local overheating regime when the Q_{in} increases.

(4) Regime IV: Overheated boiling regime

When the Q_{in} increases further, the condensing liquid flowing on the inner wall of the heat pipe fails to return to the bottom of evaporator. It is completely evaporated on the way back or it is entrained by the rapid vapor uprush due to the large evaporation rate. The multiphase flow inside the heat pipe in this regime is also similar with the annular gas-liquid counter-current flow, but the flow path is shorter than the one in regime III, as shown in the embedded sketches of Figure 3c and Figure 3d. Due to the lack of wetting by the returned liquid, the temperature of the bottom becomes overheated and much higher than that in the wetting section (Figure 3d). The further increase in Q_{in} raises the difficulty in the return of the condensed liquid, leading to the spreading of the overheated region from the bottom up. Therefore, the inflow heat cannot increase anymore with the increase of Q_{in}. The coefficient of heat transmission decreases once the overheating occurs, as shown in Figure 4. This overheated boiling may be controlled by dry-out of liquid or the entrainment limit. The controlling mechanism still needs further in-depth research.

3.2 Filling height

When the filling height is 6 m, the variations of flow regimes with inflow heat are obvious, which are reflected in the distribution and evolution of surface temperature, as discussed in Section 3.1. In comparison, Figure 6 shows the surface temperature of the heat pipe in different regimes when the fill height is 2 m. Figure 7 shows the temperature distribution of super-long heat pipe with water as

working fluid when the fill heights are 2 m and 4 m. As shown in these figures, when the fill height decreases, the changes in surface temperature of the first three regimes become less obvious. It must be noted that different from the normal size heat pipe, in which geyser boiling does not occur for the fill ratio lower than 30% [18], the geyser boiling phenomenon occurs even when the fill ratio is just 10% in super-long heat pipe. This indicates that geyser boiling is a more common phenomenon in super-long heat pipe than normal size heat pipe.

As can be seen in Figure 5, the temperature difference due to the liquid pool reduces when the fill height decreases. The periodic fluctuation in the case of FH = 2 m is much less significant compared to the case of FH = 6 m, while the GBP boiling regime does not occurs. The reason may be that the long bubble cannot form before the bubble groups reach the gas-liquid level due to the small liquid height. Consequently, the first three regimes does not distinguished in the case of smaller fill height. Moreover, the temperatures of heat pipe are more uniform before the heat pipe enters the overheated boiling regime because of the negligible influence of the liquid pool. In addition, the overheating of the super-long heat pipe with water as working fluid occurs at Q_{in} = 200 W when FH = 2 m, Q_{in} = 300 W when FH = 4 m, Q_{in} = 350 W when FH = 6 m,and Q_{in} = 400 W when FH = 10 m. This indicates that the decrease in FH results in the earlier occurrence of the overheated boiling regime and smaller maximum heat outflow.

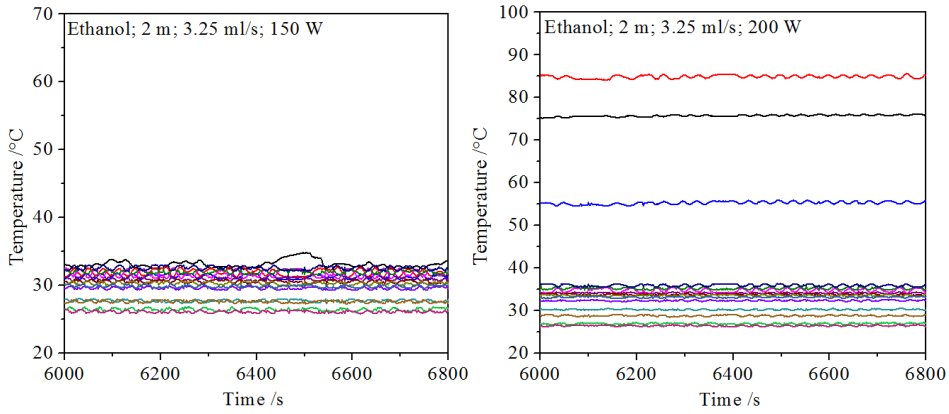

Figure 5: The flow regime along with the heat load increase (2 m)

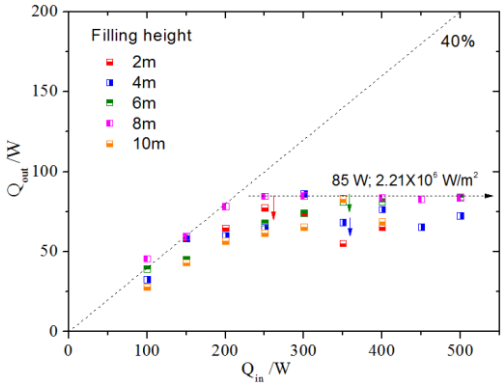

Figure 6: The thermal conductivity

3.3 Coolant temperature

Figure 7 shows the heat transmit performance of super-long heat pipe with ethanol as working fluid in different coolant flow rates when FH=6 m. As can be seen, the increase of coolant flow rates increase the outflow heat before around 300 W where the evaporator begins to be overheated. The maximum outflow arises from 67 W when v_c=2.1 g/s to 85 W when v_c=3.25 g/s and 98W when v_c=4.1 g/s . The flow regimes also show some differences with the coolant flow rate. The geyser boiling regime begins since Q_{in}=100 W when v_c=2.1 g/s, Q_{in}=150W when v_c =3.25g/s, and Q_{in}=200W when v_c =4.1 g/s. The intensity of GBP also decrease along the coolant flow rate increase. It is indicated that the increase of coolant flow rate can restrain the occurrence of geyser boiling phenomenon.

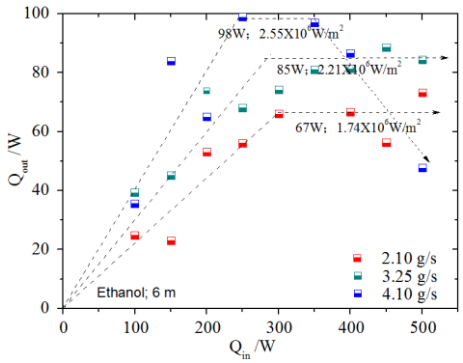

Figure 7: The effect of the velocity of the coolant water

The coolant mass flow rate has no much effect on the inflow where overheated boiling begins, while it arise the outflow heat when the overheated boiling happens, as show as Figure 7. However, along with the inflow heat increasing, the outflow heating in high coolant flow rate begins to drop fast, while the outflow heat hold steady when the coolant flow is low.

3.4 Working fluid

Figure 8 shows the heat transmit performance of super-long heat pipe using water and R134a as working fluid. The heat pipes are actually working in different regimes even in the same inflow heat for these two kinds of fluid. In the cases Q_{in} between 150~300 W, the heat pipe with water is working in the nucleating pool boiling regime, while the one with ethanol or R134a is working in the geyser boiling or evaporation film boiling regimes. Thus the one using ethanol performs better. In the case Q_{in} > 300W, the heat pipe with ethanol or R134a is working in overheated boiling regime, while the one with water just begin to working in geyser boiling or evaporation film boiling regimes. Thus the one using water performs much better. Though the heat pipe using ethonal and R134a has similar regime range, but ethanol show slightly better performance. For one thing, the performance of the heat pipe using R134a is easily effected by the filling height, and drop sharply when the inflow heat is more than 300 W, though the temperature does not show overheated. It should be because of the high density, the small latent heat and low critical temperature (T_{crit} of R134a is 91℃, while the temperature in 350 W is around 75℃).

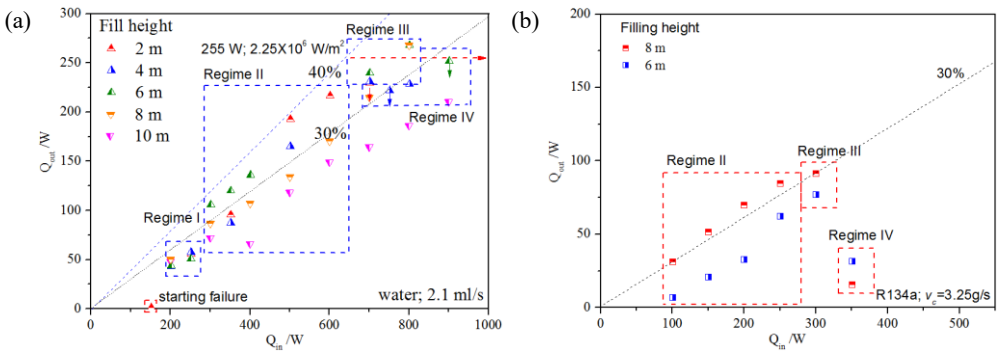

Figure 8: Performance of water and R134a

It is also illustrated that the limitation of heat transmit of super-long heat pipe is about 85 W for ethanol as working fluid, and about 250 W for water. As recommended in reference, the below two equations are used for calculating the maximum heat flux of heat pipe due to the boiling limit and the entrainment limit.

Boiling limit [19] $$Q_{\max} / S = 0.12 H_{lv} \left(\rho_v\right)^{0.5} \left[\sigma g \left(\rho_l - \rho_v\right)\right]^{0.25} \quad (4)$$

Entrainment limit [16, 20] $$Q_{\max} / A = f H_{lv} \left(\rho_v\right)^{0.5} \left[\sigma g \left(\rho_l - \rho_v\right)\right]^{0.25} \quad (5)$$

where Q_{max} is the maximum heat outflow, H_{lv} is the specific latent heat of vaporization, A and S is the cross-sectional area and the surface area of evaporator, ρ_l and ρ_v are the density of the vapor and liquid, and f is the empirical coefficient. It is uncertain that which limitation is restricting the maximum heat flux up to now. However, the maximum rate of heat transfer due to both these limitation is linear to the function of physical properties $H_{lv}\left(\rho_v\right)^{0.5}\left[\sigma g\left(\rho_l - \rho_v\right)\right]^{0.25}$. Assuming that the maximum heat outflow of the two heat pipe is controlled by the same limitation, then

$$\frac{Q_{\max}^{H_2O}}{Q_{\max}^{C_2H_5OH}}=\frac{H_{lv}^{H_2O}}{H_{lv}^{C_2H_5OH}}\left[\left(\frac{\rho_v^{H_2O}}{\rho_v^{C_2H_5OH}}\right)^2\frac{\rho_l^{H_2O}}{\rho_l^{C_2H_5OH}}\frac{\sigma^{H_2O}}{\sigma^{C_2H_5OH}}\right]^{0.25} \quad (6)$$

When the heat pipe using water, ethanol and R134a as working fluid reach limit of heat transfer, the temperature is about 75, 50 and 67 degree respectively. At these temperatures,

$$H_{lv}^{H_2O}=2320.57kJ/kg;\rho_v^{H_2O}=0.2422kg/m^3;\rho_l^{H_2O}=974.815kg/m^3;\sigma^{H_2O}=63.6mN/m$$

$$H_{lv}^{C_2H_5OH}=891.3kJ/kg;\rho_v^{C_2H_5OH}=0.5114kg/m^3;\rho_l^{C_2H_5OH}=763.111kg/m^3;\sigma^{C_2H_5OH}=19.9mN/m$$

$$H_{lv}^{R134a}=143.3kJ/kg;\rho_v^{R134a}=80.1kg/m^3;\rho_l^{R134a}=1069.1kg/m^3;\sigma^{R134a}=2.98mN/m$$

Therefore,

$$Q_{\max}^{H_2O}/Q_{\max}^{C_2H_5OH}\approx 2.5472 \quad (7)$$

$$Q_{\max}^{R134a}/Q_{\max}^{C_2H_5OH}\approx 1.4 \quad (8)$$

Depending on the experimental result, we have

$$Q_{\max}^{H_2O}/Q_{\max}^{C_2H_5OH}=250/85=2.94 \quad (9)$$

$$Q_{\max}^{R134a}/Q_{\max}^{C_2H_5OH}=98/85=1.15 \quad (10)$$

The deviation of two value is about 20%, which may come from the deviation of actual saturation temperature. This comparison indicates that the limit of heat transfer of heat pipe is partly applicable to the super-long heat pipe, though the empirical coefficient may be different. The fill height and coolant may also change the saturation temperature and further affect the maximum rate of heat transfer. Thus, the heat flux of rock layer should be considered carefully before the determination of working fluid, in order to make sure it works in the good performance regime.

4. CONCLUSION

In conclusion, a systematic experiments have been conducted to measure the heat transmit performance and surface temperatures distribution and evolution of a super-long heat pipe (L=40m，D=7mm). It is found that with the increase of inflow heat, the phase-change flow inside the super long heat pipe changes in turn as below:

(1) nucleating pool boiling regime in which the effect of liquid pool is significant;

(2) geyser boiling regime in which the surface temperature show periodic fluctuation;

(3) evaporating boiling regime in which the temperature distribution is relatively uniform in space and time;

(4) overheated boiling regime in which the bottom of heat pipe is seriously overheated.

The heat pipe show the best heat transmit efficiency in evaporating boiling regime, and the next is geyser boiling regime. The heat transmit efficiency is relatively low when it works in nucleating pool boiling regime or in the overheated boiling regime. This flow regimes transition law have been found in both the super-long heat pipe using water and ethanol as working fluid, though the corresponding inflow heat is different. Due to the difference of flow regimes, water and ethanol show superiority respectively in different heat inflow rate. In addition, the transition of these flow regimes are also influenced by operation condition such as the fill height and the coolant flow rate. Therefore, the surface temperature along the super-long heat pipe can be used to identify the flow regimes for adjusting the operating parameters accurately to improve the thermal performance.

Acknowledgments

National key Research and Development Project of China [Grant No. 2018YFB1501804 and No. 2019YFB1504104], Financial support received from Chinese Academy of Sciences Strategic Pilot Project [Grant No. XDA21060700], and key laboratory of renewable energy, Chinese Academy of Sciences [Grant No. E0290302] is gratefully acknowledged.

REFERENCES

[1] K. D. K. Breede, X. Liu, G. Falcone, A systematic review of enhanced (or engineered) geothermal systems: past, present and future, *Geoth Energy,* **1**, (2013), 1-27,.

[2] C. B. H. C.E. Clark, J.N. Schroeder, L.E. Martino, R.M. Horner, Life cycle water consumption and water resource assessment for utility-scale geothermal systems: an in-depth analysis of historical and forthcoming EGS projects, Argonne National Laboratory (ANL), Argonne, IL (United States) 2013.

[3] 黄文博, 曹文炅, 李庭樑, and 蒋方明, 干热岩热能重力热管采热系统数值模拟研究与经济性分析, *化工学报,* **1**, (2020). 1-24,.

[4] F. Jiang, W. Huang, and W. Cao, Mining hot dry rock geothermal energy by heat pipe: conceptual design and technical Feasibility Study, *Advances in new and renewable energy,* **5**, (2017), 426-434.

[5] D. Reay, P. Kew, and R. McGlen, *Heat pipes: theory, design and applications: sixth edition*: Elsevier Ltd., 2014.

[6] B. Zohuri, *Heat pipe design and technology* vol. 10.1007/978-3-319-29841-2: Springer, 2016.

[7] J. Seo, I. C. Bang, and J. Y. Lee, Length effect on entrainment limit of large-L/D vertical heat pipe, *International Journal of Heat and Mass Transfer,* **97**, (2016), 751-759.

[8] *ESDU 81038 Heat pipes – Performance of two phase closed thermosyphons*: Engineering Sciences Data Unit, London, 1981.

[9] X. Wang, Y. Wang, H. Chen, and Y. Zhu, A combined CFD/visualization investigation of heat transfer behaviors during geyser boiling in two-phase closed thermosyphon, *International Journal of Heat & Mass Transfer,* **121**, (2018). 703-714,.

[10] M. K. Bezrodnyi and S. S. Volkov, Study of Hydrodynamic Characteristics of Two-Phase Flow in Closed Thermosiphons, in *Advances in Heat Pipe Technology*, D. A. Reay, Ed., ed: Pergamon, **1**, (1982), 115-123.

[11] A. A. Alammar, R. K. Al-Dadah, and S. M. Mahmoud, Experimental investigation of the influence of the geyser boiling phenomenon on the thermal performance of a two-phase closed thermosyphon, *Journal of Cleaner Production,* **172**, (2018). 2531-2543.

[12] T. F. Lin, W. T. Lin, Y. L. Tsay, J. C. Wu, and R. J. Shyu, Experimental investigation of geyser boiling in an annular two-phase closed thermosyphon, *International Journal of Heat and Mass Transfer,* **38**, (1995), 295-307,.

[13] H. Jouhara, B. Fadhl, and L. C. Wrobel, Three-dimensional CFD simulation of geyser boiling in a two-phase closed thermosyphon, *International Journal of Hydrogen Energy,* **41**, (2016), 16463-16476.

[14] H. Kuncoro, Y. F. Rao, and K. Fukuda, An experimental study on the mechanism of geysering in a closed two-phase thermosyphon., *International Journal of Multiphase Flow,* **55**, (1995), 333-348,.

[15] G. Xia, W. Wang, L. Cheng, and D. Ma, Visualization study on the instabilities of phase-change heat transfer in a flat two-phase closed thermosyphon, *Applied Thermal Engineering,* **116**, (2017), 392-405.

[16] H. Nguyen-Chi and M. Groll, Entrainment or flooding limit in a closed two-phase thermosyphon, *Journal of Heat Recovery Systems,* **1**, (1981), 275-286.

[17] F. E. Andros, Heat transfer characteristics of the two-phase closed thermosyphon (wickless heat pipe) including direct flow observation, Tempe. Dept. of Mechanical and Energy Systems Engineering., Arizona State Univ.1980.

[18] S. H. Noie, M. R. S. Emami, and M. Khoshnoodi, Effect of inclination angle and filling ratio on thermal performance of a two-phase closed thermosyphon under normal operating conditions, *Heat Transfer Engineering,* **28**, (2007), 365-371.

[19] J. H. Linehard and V. K. Dhir, Extended hydrodynamic theory of the peak and minimum pool boiling heat fluxes, NASA, Washington, United States NASA-CR-2270, (1973).

[20] M. K. Bezrodnyi and S. S. Volkov, Study of hydrodynamic characteristics of two-phase flow in closed thermosiphons, *Advances in Heat Pipe Technology,* (1982), 115-123.